

Theoretical Effects of Periodic Ripple, Banana-Type Curvature and Figure Error on Capillary Focusing Performance by MATLAB Simulation

Tia Plautz

Cornell University, Ithaca, NY 14853

August 13, 2010

Abstract

A simulation was programmed in MATLAB (The MATrix LABoratory) in order to model the performance of a CHESS capillary designed to deliver a 2 μm beam size at the focus. The larger, observed beam sizes of 4-6 μm are due to defects in production. I investigated the effects of imperfections that fall into three main categories: periodic ripple, banana-type curvature and figure error. Each defect and its effects on spot size and divergence was analyzed separately by superposing an appropriate correction function onto an ideal capillary of the 2 micron design. Combinations of defects were also studied. Root mean squared (rms) statistics were calculated for each type of imperfection.

Running of the simulation shows that the number of sinusoidal ripples corresponds to the number of bright rings visible on a screen downstream from the capillary. As the amplitude of ripple increases, the spot size increases linearly, and likewise, as ripple number increases, spot size also increases linearly. Generally, ripple amplitude is likely less than 50 nm for a period of 3.33 mm (slope error $\approx 60 \mu\text{rad}$) and for our best capillaries, ripple amplitude is likely less than 30 nm for a period of 4 mm (slope error $\approx 30 \mu\text{rad}$). For designated “good” capillaries, although ripple is present, it contributes less to broadening of the focal spot than do other defects, namely curvature and figure error.

Curvature seems to contribute most to the increased spot size and is related to the the spot size linearly by $\frac{1}{R}$ where R is the radius of curvature. Curvature causes rays reflecting from the more curved surface to be reflected at a higher angle and with a higher divergence than rays reflecting from the less curved surface which creates non-uniform, non-concentric rings in the far field. Curvature also shifts the focal spot off of the ideal axis of the capillary. As compared with a very slight curvature, $R = 500 \text{ m}$ which produces a spot size of 0.5-2 μm for low amplitude ripple (10-30 nm) and 2.5-3.5 μm for higher amplitude ripple(40-60 nm), moderate curvature $R = 50 \text{ m}$ produces spot sizes four times larger for low amplitude ripple, and twice as large for higher amplitude ripple. Capillaries

G1_mr7f15_01 and G1_mr10_07 were calculated to have radii of curvature $R = 68$ m and $R = 35$ m respectively.

Cubic figure error functions for the diameters of capillaries G1_mr7f15_01 and G1_mr10_07 were fitted using a simple MATLAB script `fig_err_analysis`. As compared with the ideal model of G1_mr7f15_01 which produced a simulated spot size of 0.03-0.04 μm , a figure error-corrected model (no ripple or curvature corrections) produced a spot size of 1.1 μm . Figure error corrections shift the focus of the capillary farther from the capillary tip, and decrease the divergence. Expected figure errors for capillaries G1_mr7f15_01 and G1_mr10_07 were calculated from the diameter profile data to be 0.75% and 2.6% deviations from the theoretical models at the tips of the capillaries respectively. Upon analyzing the simulation, it was found that figure errors at the tip more likely corresponded to 0.33% and 0.31% deviations from the theoretical models respectively.

In conclusion, banana-type curvature appears to contribute most to increasing the spot size of a capillary. Working to minimize this type of defect would greatly improve the average focusing performance of CHESS capillaries.

1 Introduction

Optics studies the behavior and properties of light. Geometric optics is a practical application of optical physics that treats light as a collection of rays that travel in straight lines and bend at interfaces of different media [1]. An optic is used to exchange divergence for size, and specifically, a capillary is used in order to achieve small beam sizes and high gains. Theoretical gain calculations expect that capillaries should be able to produce flux densities of hundreds to thousands of times greater than than the original collimated beam.

As the samples scientists wish to study decrease in size, smaller beams are needed to probe the structure of the sample, be it a crystal, a protein or a virus. Optical capillaries are used at CHESS in order to achieve beam sizes small enough to suit the needs of researchers. The capillaries of interest are of the single-bounce variety which are elliptical in geometry: an x-ray leaving a source located at one focus of the ellipse will be redirected toward the other focus of the ellipse in a single bounce (Fig. 1). The ellipses on which the capillaries are modeled can typically have semi-major axes of about 15-17 m and semi-minor axes of 1-2 mm, rendering them very long and skinny. One of the reasons why this is essential is because x-rays only reflect from surfaces at very small, glancing angles – at angles greater than 3.5 mrad (~ 0.2 degrees) reflectivity goes to zero for 10 keV x-rays. Monocapillaries are desirable to other methods of beam-width reduction because they are nearly 100% efficient, that is, all rays incident on the capillary are transmitted with little to no attenuation, their focal lengths are on the order of a few centimeters which provides a reasonable working length, and the divergence is easily controllable using the elliptical geometry of the capillary.

The elliptical geometry of the capillary determines the spot size and the divergence of the beam. A beam incident on the capillary from a fixed source reflects off the inner surface of the capillary

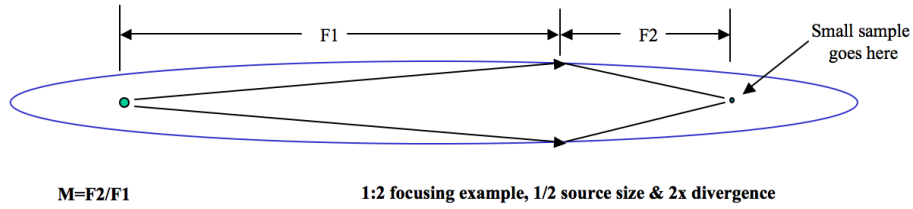


Figure 1 – The geometry of an ellipse is such that a ray emitted from a source located at one focus of the ellipse will be redirected toward the other focus in a single bounce.

through the focus. At the focus, a demagnified image of the source appears. Since our source is not ideal, and rather has a finite area, the focused source appears as a focal “spot” with a finite area scaled by a magnification constant M (Fig. 1).

All capillaries are manufactured at CHESS using a precision glass puller that stretches high quality glass tubing into elliptical tapers using a conservation of mass relationship [2]. The puller operates by applying constant tension to the glass tube while rotating it in a furnace. Deviations from the theoretical shape of the capillary occur due to imperfections in the manufacturing of the capillary, as well as defects in the original glass tubing. These imperfections can critically affect the performance of a given capillary.

2 Purpose and Research Goals

Monocapillary optics have been able to consistently produce spot sizes between 5 and 10 μm in diameter and have been successfully applied in x-ray crystallography, small angle x-ray diffraction, macromolecular imaging and x-ray fluorescence. In the near future we hope to apply our optics in microcrystallography, microfluidics and micro-Laue diffraction experiments. There are several limitations we face in reducing our spot size down to the level needed for these experiments. One of these limitations is that there is currently no reliable method to non-destructively observe or measure the shape of the inner surface of a capillary. The current method used to gather information about the inner surface of the capillary utilizes lasers which image the outer profile of the capillary. We often assume that a fixed ratio (4:1 - 10:1) of outer diameter to inner diameter is essentially preserved. A second, more experimental method analyzes slope errors in the far-field image using the “small spot method” [3]. The limitations of this second method is that our equipment does not yet seem to provide high enough resolution for very precise metrology, and it also requires a large amount of synchrotron time.

One purpose of devising this simulation was to learn about the inner surface of the capillaries in a theoretical and non-destructive manner. The simulation uses a ray-tracing technique which illustrates the behavior of a capillary subject to various model defects. The simulation is able to model three major types of capillary imperfections including periodic ripple, banana-type curvature and figure

error, as well as random or pseudorandom noise. The simulation was used to learn about the ways each of these types of errors affected the performance of the capillary. A second application of the simulation was to try to learn more about our fabrication process and how well we are doing at minimizing drawing errors.

3 Capillary Imperfections

There are three primary categories into which capillary imperfections fall: periodic ripple (hereafter simply “ripple”), banana-type curvature (hereafter simply “curvature”) and figure error. These three types of imperfections are illustrated in Fig. 2.

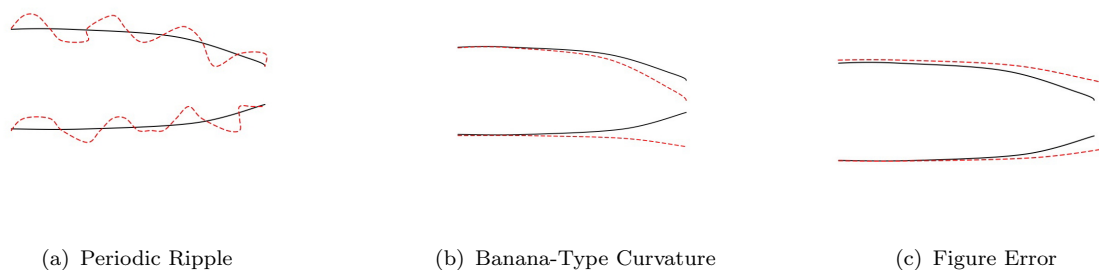


Figure 2 – Note: Images are greatly exaggerated. (a) Ripple on the inner surface of the capillary is sinusoidal and periodic. (Not represented: simulated ripples are perfect sinusoids.) (b) Curvature describes the bending of a capillary into a banana shape by increasing curvature of one surface of the capillary and decreasing the curvature of the opposite surface. (c) Figure error describes the characteristic flattening of the capillary tip by a systematic error of the capillary puller

3.1 Ripple

Ripple is best described as an inner surface defect that is characteristically periodic, and modeled as a sine curve on the inner wall of the capillary. Ripple was first hypothesized to be the cause of alternating bright and dark rings in the far field images of capillaries. It is a fundamental characteristic of ripple that the phase of the ripple is the same on both the top and bottom surfaces in the model.

3.2 Curvature

Curvature represents the bending of a capillary into a banana shape. In general, the innermost ring on the far field screen is caused by reflection from the base of the capillary, while the outermost ring on the far field is due to reflection from the tip of the capillary (Fig. 3(a)). If the centerline through the tip of the capillary is offset from the centerline through the base of the capillary by some angle, the outermost ring and the innermost ring will be non-concentric. The radius of curvature (Fig. 3(b)) can be calculated by determining the angular separation between the centers of the inner and outer

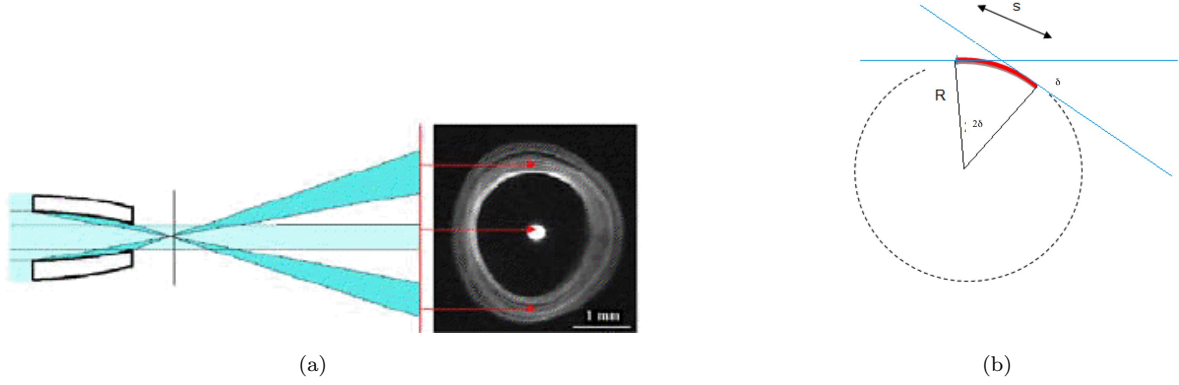


Figure 3 – (a) The innermost ring on the far field screen is due to reflection from the base of the capillary while the outermost ring is due to reflection from the tip. (b) The radius of curvature R describes how bent a capillary is.

rings and using the relationship

$$\delta = \frac{d}{2L} \quad (1)$$

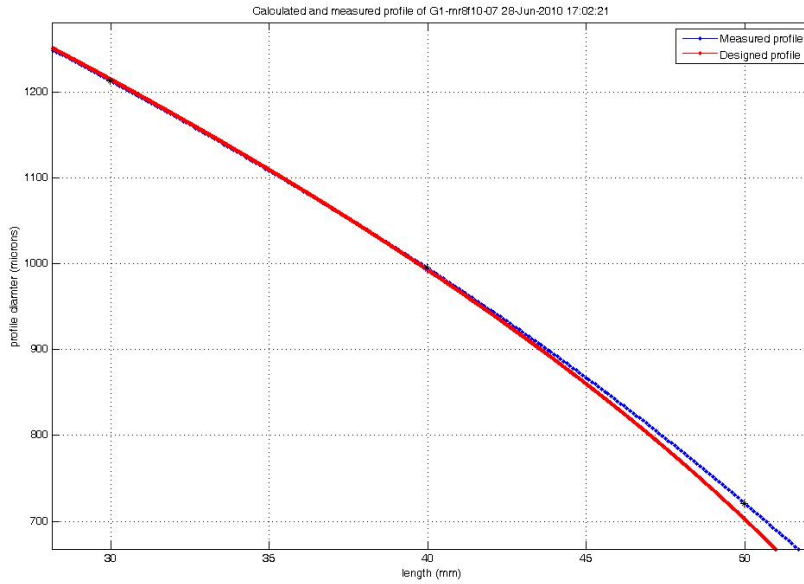
where d is the displacement of the centers on the far field, L is the distance to the far field and δ is the angle of offset between the centerline through the base of the capillary and the centerline through the tip of the capillary. Then applying the basic relationship $s = r\theta$ and the small angle approximation we find simply that

$$R = \frac{\ell}{2\delta} \quad (2)$$

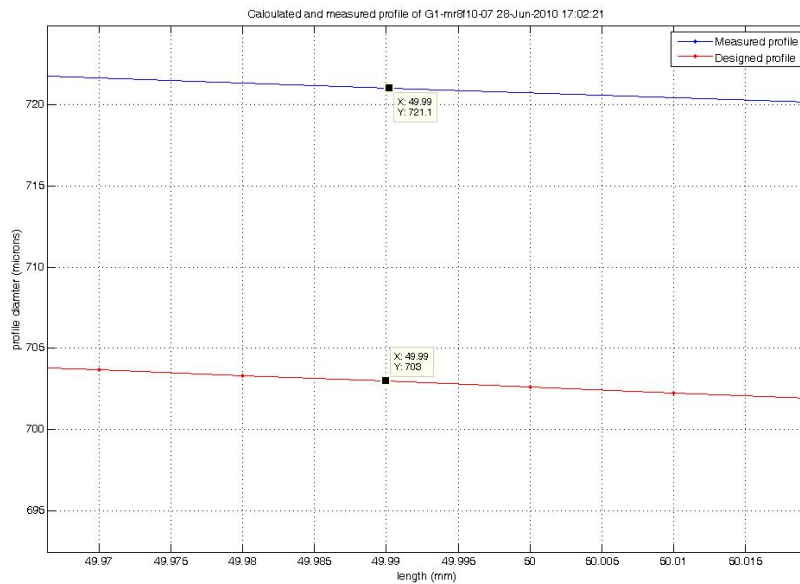
where ℓ is the length of the capillary. Curvature results in increasing the curvature of one half of the capillary (the top half shown in Fig 2(b)) and decreasing the curvature of the other half relative to the ideal ellipse.

3.3 Figure Error

Figure error describes the characteristic flattening of the capillary tip as a result of a systematic error of the capillary puller. These errors are documented mainly by profile scans of the centerline and diameter of the capillaries and can be calculated by finding the functional difference between the theoretical profile of the capillary and the observed profile of the capillary (Fig. 4). It was hypothesized that figure error would mainly contribute to shifting focus of the capillary farther from the capillary tip and to slightly reducing the divergence of the capillary. Figure errors have been estimated from diameter profile scans to be between 0.75% and 3% of the theoretical diameter (0.37-1.5% of the theoretical radius) and are defined to be symmetric around the capillary.



(a) Full length of capillary



(b) Tip of capillary

Figure 4 – Plots of the theoretical (red line) and observed (blue line) profiles of capillary G1_mr8f10.07. The figure error is calculated by subtracting the theoretical profile function from the observed profile function. (a) shows the profile of the full length of the capillary (plotted between positions 30 mm and 50 mm in the scan), while (b) zooms in on the tip of the 2 μm capillary design illustrating the maximum difference of the observed curve from the theoretical curve. Theoretical tip coordinates: ($x=50\text{mm}$, $y=703\mu\text{m}$). Observed tip coordinates: ($x=50\text{mm}$, $y=721.1\mu\text{m}$).

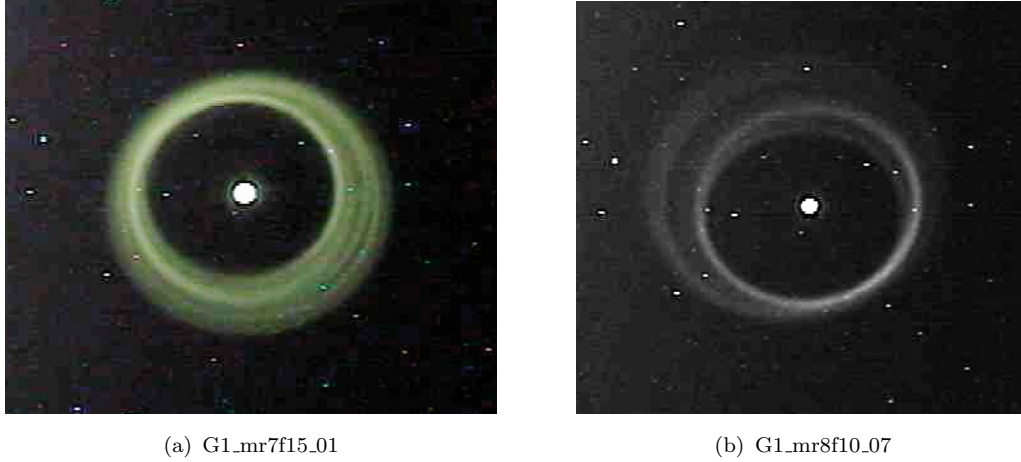


Figure 5 – (a) Far field image of capillary G1_mr7f15_01 at 780 mm, measured focal length=17 mm, measured horizontal/vertical divergence=5.95/6.35 mrad. (b) Far field image of capillary G1_mr8f10_07, measured focal length=11 mm, measured horizontal/vertical divergence=6.15/7.44 mrad. Note: Diameter of outer rings are about 5 mm.

4 Data Analysis and Results

After repeated running of the simulation it became clear that, as expected, all capillary imperfections increased the spot size of the capillary, but certain imperfections affected the spot size less than others. In addition, each imperfection had characteristic effects on the far field. Using the observed trends it was possible to reasonably reconstruct two capillaries G1_mr7f15_01 and G1_mr8f10_07 (Fig. 5) which were both determined to be “good” capillaries during our beam run July 17-20, 2010.

4.1 The Ideal Capillary

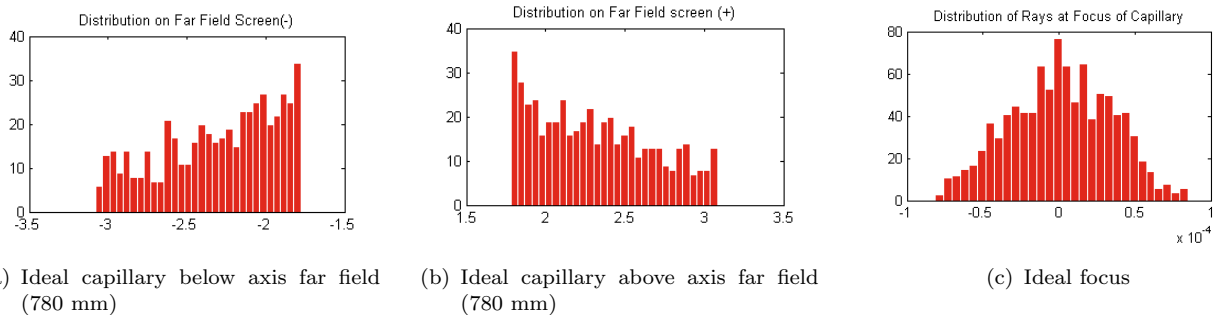


Figure 6 – The figures above are derived from modeling 1000 rays incident on an ideal capillary from a 1 mm source located ~ 35 m from the capillary. Horizontal axis is in millimeters. (a),(b) The far field is symmetric above and below the axis of the capillary. A greater number of rays strike the far field screen closer to the axis because there is a higher cross-sectional area at the base. (c) The focal spot of a simulated ideal capillary has an rms value between 0.03 and 0.04 μm and is Gaussian in shape.

A simulated ideal capillary (capillary length=20 mm, focal length=10 mm), given a 1 mm source

at a distance of 35 m has a spot size on the order of $.01 \mu\text{m}$ (10 nm)¹. The ideal spot has a finite area because our source is not an ideal point source but rather has a height of about a millimeter (this can be modified in the simulation such that it models the exact source size)². Figs. 6(a) and 6(b) show the distribution of rays in the far field and at the focus for an ideal capillary. Notice that more rays strike the far field screen closer to the axis. This is because the cross sectional area of the capillary is larger at the base and thus rays are probabalistically more likely to intersect the capillary closer to the base. Furthermore, the distribution of rays at the focus of the capillary is, as one would expect a Gaussian distribution where the largest number of rays pass very close to the focus of the ellipse, then taper off gradually and symmetrically above and below the ideal axis.

4.2 Effect of Ripples

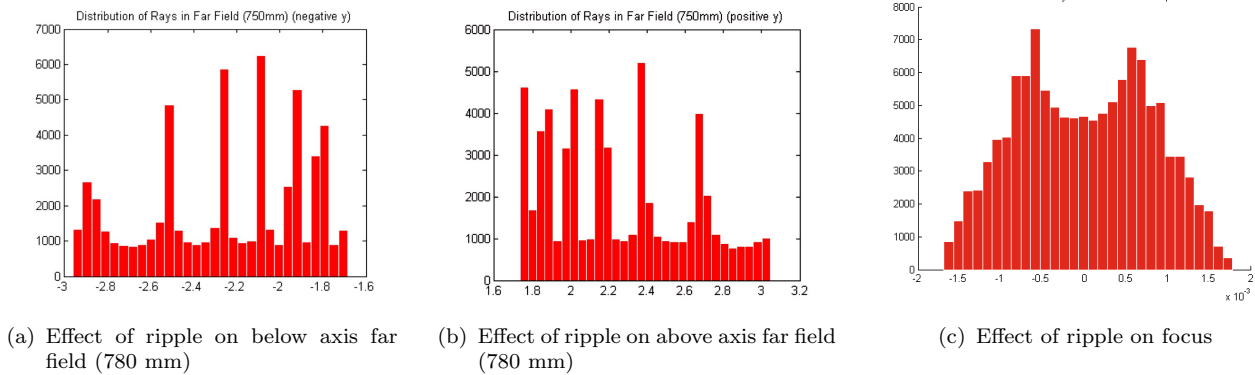
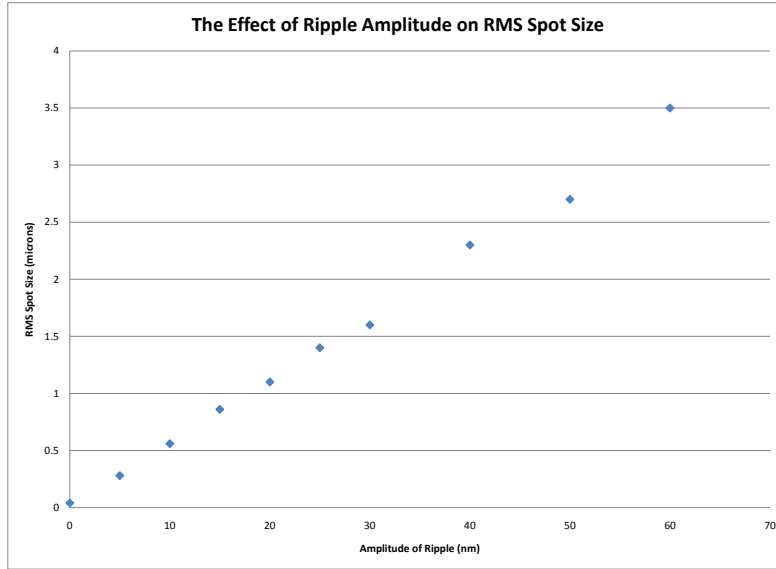


Figure 7 – The figure above models 120,000 rays incident on a capillary with ripple, amplitude=15 nm, period=3.33 mm corresponding to $60 \mu\text{rad}$ slope error (source size=1 mm). Horizontal axis is in millimeters. (a),(b) the far field image is still somewhat symmetric above and below the axis of the capillary. 6 distinct peaks are characteristic of the 6 sinusoidal ripples along the inner surface of the capillary. (c) The distribution of rays at the focus for a capillary with ripples changes from the Gaussian we observed in the ideal capillary to a bimodal distribution. Note that the horizontal scale differs by a factor of 10 from 6(c).

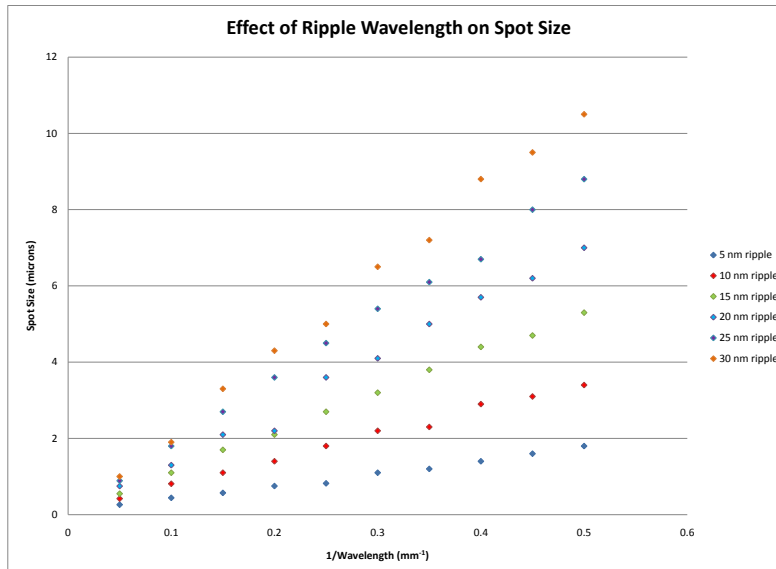
It was hypothesized that the bright and dark rings in the far field (visible in Fig. 5(a)) are due to periodic ripple on the inside surface of the capillary. Indeed, the simulation showed that certain bands are more illuminated than others when a ripple is added (Fig. 7). Additionally, the number of bright bands in the far field corresponds directly to the number of ripples on the inner surface of the capillary. This occurs because as a ray strikes the portion of a ripple that is more convex it is deflected at an angle greater than it would have been had it struck an ideal capillary surface. Conversely, if a light ray strikes the more concave part of a ripple, it is deflected less in the far field. In addition, rays striking the top surface of the capillary are *more likely* to intersect the capillary when the slope of the

¹The “ideal” *designed* capillaries have a spot size of $\sim 2 \mu\text{m}$

²In the geometric approximation, an ideal point source would yield an ideal point focus, that is, the focus would have nearly zero size

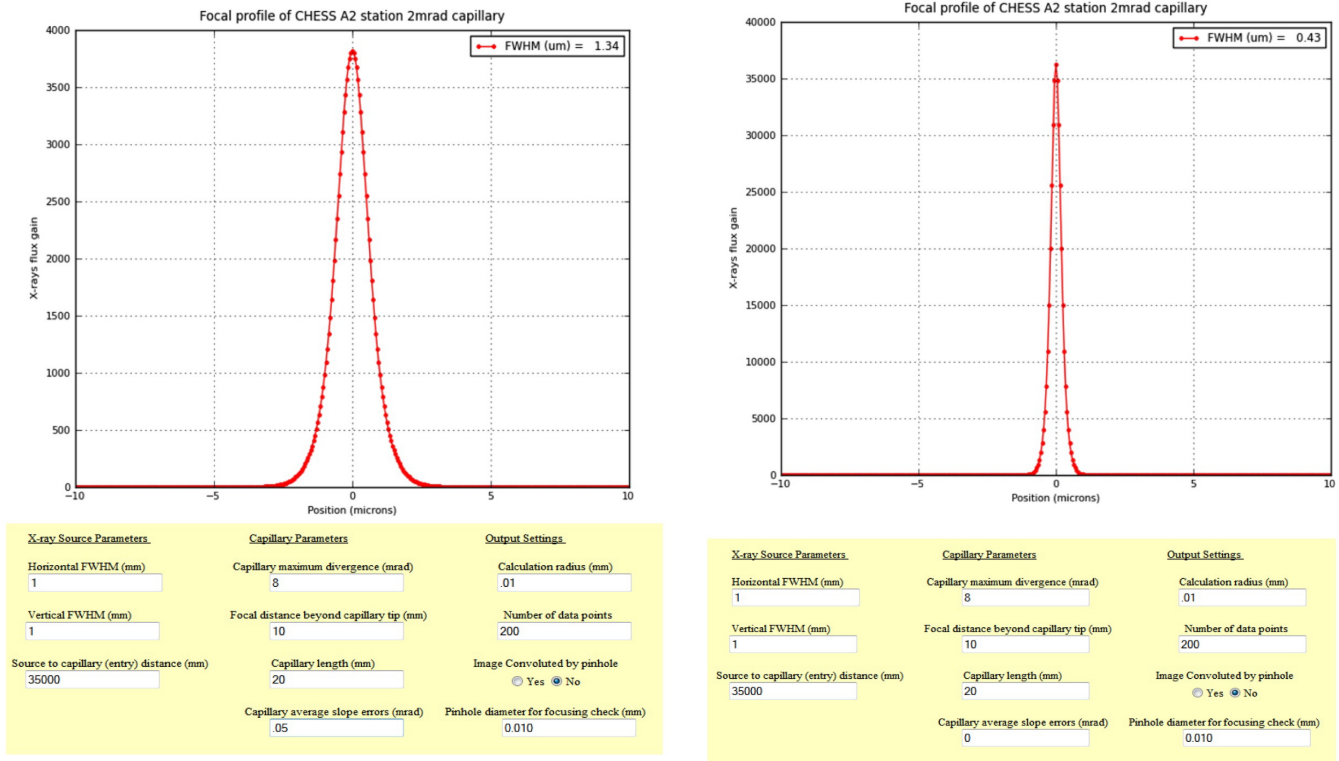


(a)



(b)

Figure 8 – (a) RMS spot size increases linearly with increasing ripple amplitude. Minimum spot size for a simulated ideal capillary = 0.03 μm . (b) RMS spot size increases linearly with $1/\lambda$.



(a) Corrected for slope error

(b) No slope error

Figure 9 – Theoretical gain curves for 2 micron capillary design produced by Rong Hwang’s Capillary Profile Calculator. Both curves are for a 1 mm source size at a distance of 35 m. (a) Displays the gain curve assuming a $50 \mu\text{rad}$ slope error. (b) Displays the gain curve if no slope error is present (i.e. a perfect capillary).

sinusoid is negative and similarly, rays that strike the bottom surface of the capillary are more likely to intersect the capillary when the slope of the sinusoid is positive.

A model of 120,000 rays incident on a 20 mm capillary, focal length=10 mm, with ripple amplitude=15 nm, period=3.33 mm (slope error= $18 \mu\text{rad}$) is available in Fig. 7. Figs. 7(a) and 7(b) show the distribution of rays in the far field above and below the axis of the capillary, respectively. When such a large number of rays is plotted, the output shows a smooth distribution. The rays are equally distributed about most of the bins except for six peaks which represent intensity peaks corresponding to the six ripples on the inner wall of the capillary.

In addition, the histogram plot of the focus (Fig. 7(c)) shows that the distribution of rays changes from the expected Gaussian distribution which we saw for an ideal capillary to a bimodal distribution. Since the rays are more likely to strike a more convex surface of the capillary, they are more likely to be deflected either above or below the focus of the ellipse than they are to be deflected right through the focus.

The next question that arose was, on what order are the amplitudes of the ripples that we are working with? Prior to modeling, it was guessed that ripple amplitudes were on the order of about

a micron, however, simulation showed that this amplitude ripple was far too big and rather, the amplitude of the ripples must be on the order of a couple tens of nanometers, likely less than 50 nm in general, and for a “good” capillary, less than 30 nm. An analysis showed that increasing the amplitude of the ripple increased the rms value of the focal spot linearly. This data is plotted in Fig. 8(a) for ripples of 0 to 60 nm (corresponding to slope errors of 0 to 70 μrad). Fig 8(b) shows that spot size is linearly related to the inverse of the wavelength of the ripple³. Notice that as the amplitude of the ripple increases, so does the slope of the line indicating that as we expect, keeping wavelength constant and increasing the amplitude of the ripple also increases the spot size.

As a reliability check, a 50 μrad ripple correction (amplitude=40 nm, period=3.33 mm), and a 50 μrad curvature ($R=200$ m), were each evaluated in order to check the model’s agreement with Rong Hwang’s Capillary Profile Calculator⁴ which predicts a spot size of 1.34 μm for the 8 mrad design assuming 50 μrad of slope error (Fig. 9). The ray tracing approach produced a spot size of ~ 2 μm for the ripple correction, and ~ 1 μm for the curvature correction, both of which are in good agreement with Rong Hwang’s calculator.

4.3 Effect of Curvature

While curvature is noticeable in both images Figs. 5(a) and 5(b), it is most clear in the latter. In this image we see two distinct rings, an inner and an outer whose centers are displaced by a measurable amount (in this case $\alpha \approx 577$ μrad). It became evident in running the simulation, that superposing a negatively sloped curvature function on the capillary caused more rays to intersect the top half of the capillary, and fewer rays to intersect the bottom half. Additionally, since the top half the capillary was more curved, the rays were reflected at higher angles which caused the focus of the capillary to shift down below the ideal axis. Fig. 10(c) shows a cross section of the focus of a capillary with 15 nm ripple and a 75 m radius of curvature. Notice that all the ray crossings occur below the zero axis and that the center of mass of the focus is around -7 μm . As we’ve previously discussed, the effects of curvature on the far field are very noticeable. Rays reflecting from the more curved surface of the capillary intersect one another before the focus of the capillary while rays reflecting from the less curved surface intersect past the focus of the capillary. This causes the former to diverge by a greater amount in the far field. For a capillary with negative curvature, this results in a wider ring on the negative half of the far field and a narrower ring on the positive half (Figs. 10(a) and 10(b)).

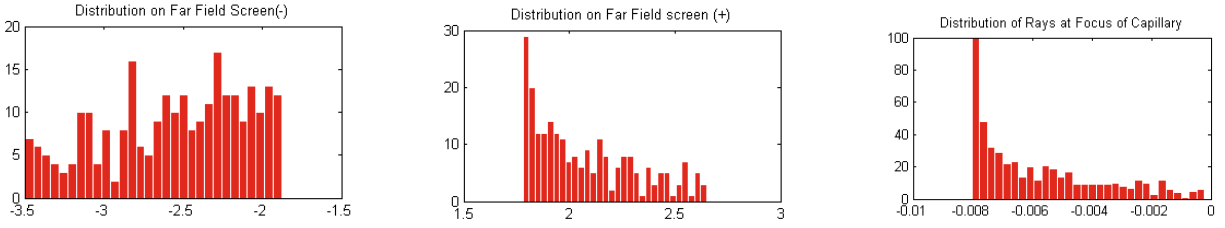
While ripple has the potential to increase spot size the fastest (Section 4.2 notes that 50 μrad of ripple produces a spot size of 2 μm while 50 μrad of curvature produces a spot size of only 1 μm), curvature seems to be our greatest limitation on our ability to achieve a 2 μm beam size⁵.

As compared with a capillary with very little curvature, $R=1000$ m (or $\delta=10$ μrad), applying a

³Another way to express this is to say that the spot size is linearly related to the *number* of ripples along the inner surface of the capillary

⁴Rong Hwang’s Capillary Profile Calculator is available online at <http://glasscalc.chess.cornell.edu/imageprof.shtml>

⁵This is because we are not consistently dealing with 50 μrad ripple, but we *are* dealing with curvatures of 200-300 μrad .



(a) Effect of curvature on below axis far field (780 mm) (b) Effect of curvature on above axis far field (780 mm) (c) Effect of curvature on focus

Figure 10 – These figures model 500 rays incident on a capillary with radius of curvature $R = 75\text{m}$, for source size=1mm at a distance of $\sim 35\text{ m}$. Horizontal axis is in millimeters. (a),(b) Adding negative sloping curvature correction causes the far field distribution below the axis to diverge and the far field distribution above the axis to condense. (c) Adding curvature causes the focus to shift below the ideal axis of the capillary.

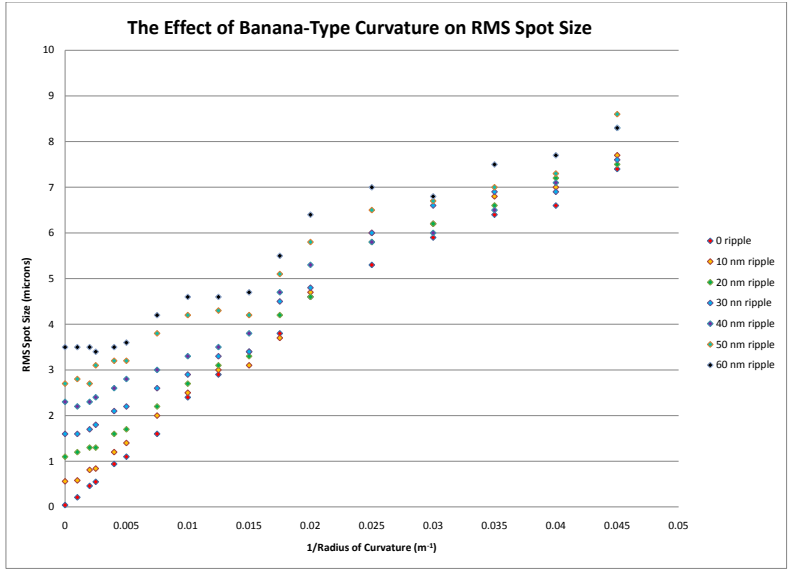
reasonable curvature of $R = 50\text{ m}$ ($\delta = 200\ \mu\text{rad}$) approximately quadruples the spot size for small amplitude ripples and more than doubles the spot size for larger amplitude ripples⁶. Fig. 11(b) shows that for low curvature ($R > 50\text{ m}$) there is a linear relationship between the observed spot size and $1/R$. Additionally, it is reasonable to note that as ripple amplitude increased, the slope of the best fit lines decreased, indicating that increased ripple amplitude decreased the effects of adding curvature, probably due to more frequently variable slope errors. Furthermore, the spot sizes for very low curvature have a wider distribution than those at higher curvature, which suggests that as curvature is increased, the amplitude of the ripple starts to make less of a contribution to the size of the spot.

The more generalized plot shown in Fig. 11(a) displays an interesting quality of curvature. It appears that the graph can be divided into two sections, quickly increasing and slowly increasing. The quickly increasing section is characteristic of curvature $R < 40\text{m}$ while the slowly increasing section is characteristic of curvature $R > 40\text{m}$. It appears that at this critical value, increased curvature seems to produce little effect. This is because when curvature gets too high, the majority of rays strike the more curved parts of the capillary, and fewer rays strike the flattened part. Eventually, curvature gets so high that rays cannot pass through the capillary. In the intermediary time, however, the intersection of rays at the focus becomes extremely unbalanced and the deficiency in rays reflected from the less curved surface limits the amount the size of the focus can increase.

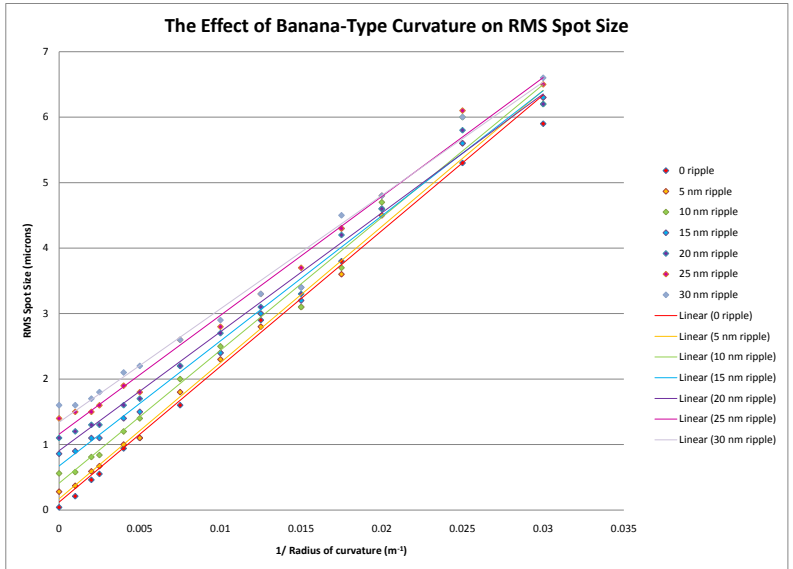
4.4 Effect of Figure Error

Figure error was perhaps the most difficult correction to analyze – determining a general, slowly increasing function that hovered around zero for for about two-thirds of the capillary’s length before increasing to a desired percentage of the ideal diameter of the capillary was non-trivial. A simple

⁶G1_mr7f15_01 (Fig. 5(a)) was calculated to have a curvature of $R = 45\text{ m}$ (corresponding to an angular displacement, δ , of $222\ \mu\text{rad}$ between the axis through the base of the capillary and the axis through the tip), while G1_mr8f10_07 (Fig. 5(b)) was calculated to have a curvature of about $R = 35\text{ m}$ ($\delta = 286\ \mu\text{rad}$). Both of these capillaries were considered “good.”



(a)



(b)

Figure 11 – (a) Simulation data for 0 curvature to a radius of 22m for ripples of 0 to 60 nm. (b) plots simulation data for 0 curvature to a radius of 33 m for ripples of 0 to 30 nm. RMS spot size increases linearly with $1/R$.

MATLAB script `fig_err_analysis` was written, which reads in the data files of the theoretical capillary diameter profile and the observed capillary diameter profile, then fits a cubic function to each and subtracts the two functions to find the difference function. This correction function is then added to the top half of the capillary and subtracted from the bottom half of the capillary keeping the figure symmetric about the capillary’s axis. Because the data for figure errors is capillary specific it was not possible to do statistics on the figure error data, however, when applied to capillaries G1_mr7f15_01 and G1_mr8f10_07, it became clear that the calculated figure errors were indeed too great.

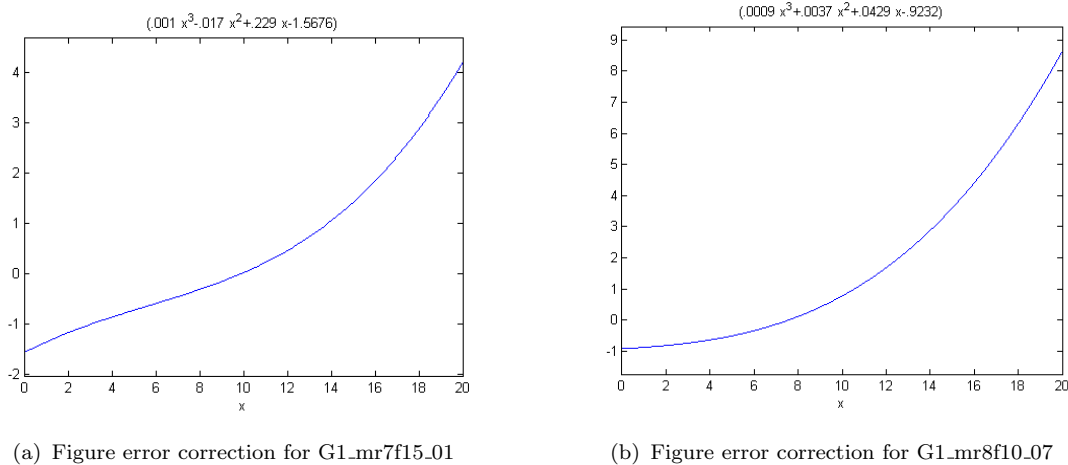


Figure 12 – MATLAB script `fig_err_analysis` reads in data files of theoretical and observed capillary diameter profiles and calculates the difference between them to give the figure error function. The above horizontal axes are in millimeters (along the capillary length), and vertical axes are in microns.

The calculated figure error functions for G1_mr7f15_01 and G1_mr8f10_07 are given in Fig. 12. When the function plotted in 12(a) was superposed on the capillary model, the focal length increased to 20 mm and the divergence of the capillary was reduced to 4.2 mrad, (about 60% of its theoretical value). Our experimental results from G1 yielded a focal length of 17 mm and a divergence of 5.95 and 6.35 mrad in the horizontal and vertical directions respectively. This figure error function corresponded to a figure error of only 0.75% at the capillary tip. The experimentally chosen “best” capillary, G1_mr8f10_07 was calculated to have a figure error of 2.6% at the tip. After seeing the results of the simulation I became wary whether or not it was even possible for so good a capillary to have such a large figure error. As expected, when the figure error function plotted in Fig. 12(b) was superposed on the model of capillary G1_mr8f10_07, the focal length was increased to 17 mm and the divergence was reduced to 4.4 mrad, 55% of its designed value, both of which were unreasonable corrections. The experimentally measured focal length of this capillary was 11 mm and the divergence was 6.15 and 7.44 mrad along the horizontal and vertical axes respectively.

Both of these figure error functions appeared to be reasonably shaped but the maximum values of these functions at the capillary tip were clearly too high so the simulation was run for several multiples

of each figure error. For capillary G1_mr7f15_01 a multiple of $\frac{1}{3}$ was sufficient to make the output of the simulation more reasonable, decreasing the focal length to 16 mm and increasing the divergence to 5.3 mrad, which is still on the low side but slightly more reasonable. This figure error corresponded to a .33% difference between observed and theoretical values at the tip of the capillary. For capillary G1_mr8f10_07, a factor of $\frac{1}{4}$ was needed to reduce the focal length to a reasonable 12 mm and to adjust the divergence to 6.6 mrad. The resulting function corresponded to a 0.31% figure error at the tip.

As the figure error curve was lifted right from the optical metrology on the capillary outer wall, it was surprising that the calculated curves led to output that was so poorly representative our experimental observations.

There are several explanations as to why the calculated figure error was not correct. It is indeed possible that the reading of the diameter profile by the scanner is not entirely precise. It has been recently discovered that when the scanner is left to run on its own, taking diameter profile data for a stationary glass tube, it has a tendency to drift. This drift is highly variable and ranges from an 8 μm drift in 30 min (roughly 0.27 $\mu\text{m}/\text{min}$) to a 10 μm drift over 7 min (roughly 1.43 $\mu\text{m}/\text{min}$) and could cause erroneously high and highly variable displacement readings at the tip. A second explanation which may have more of an effect on our understanding of figure error itself is that the figure error may not be symmetric all the way around the capillary. Figure error and curvature may not be entirely independent of one another, and what we call the “flattening” of the tip may in fact be a side effect of curvature in which the more curved surface of the capillary gets stretched less than the less-curved surface, toward the end of a pull. Since our metrology only allows us to measure the diameter of the capillary by scanning its outer surface, we have no way of knowing at this time whether the figure error is in fact symmetric or not. Finally, it is also possible that toward the end of a pull we are not perfectly conserving the 10:1 ratio of the outer diameter to the inner diameter. If the ratio is increased toward the end of the pull, rendering the walls of the capillary thicker, our current metrology would calculate the inner diameter of the capillary to be bigger than it actually is.

5 Modeling Capillary G1_mr7f15_01

Capillary G1_mr7f15_01 was modeled for a source size of 0.5 mm located at 5 m from the capillary. The radius of curvature of capillary G1_mr7f15_01 was calculated from the far field image (Fig. 5(a)) to be about 68 m. Since the vertical and horizontal scales of the image are slightly different this was determined by measuring the horizontal widths of the ring, and the vertical widths of the ring separately and then using vector addition to compute the offset of the centers. The narrowest region of the ring is about .5 mm while the widest region is about 1.15 mm. The far field output of the simulation when a 68 m radius of curvature was used as a curvature correction is given in Fig. 13(a). This figure illustrates that the narrow part of the ring is 0.42 mm while the widest part of the ring is 0.55 mm which is quite a bit narrower than expected. Going back to our curvature plot (Fig. 13)

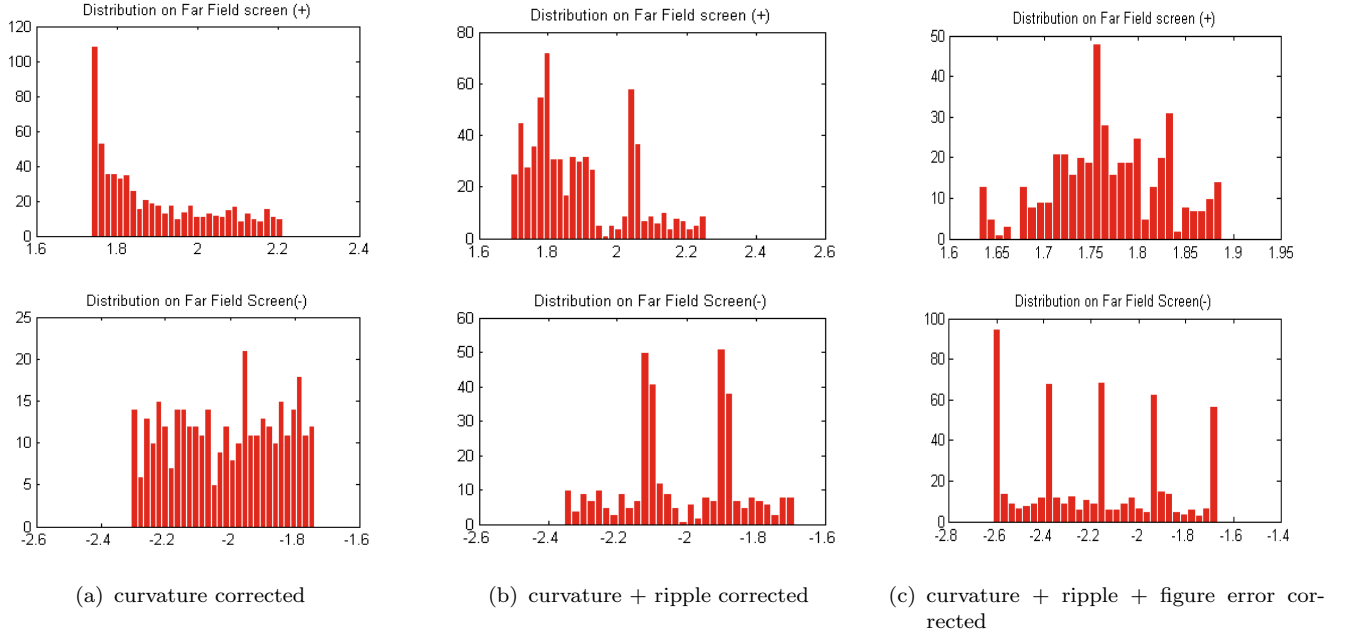


Figure 13 – Top: Distributions of rays in the far field above the capillary axis. Bottom: Distributions of rays in far field below capillary axis. This figure illustrates far-field cross sections for capillary G1_mr7f15_01, radius of curvature =68m. (a) is the cross section when only the calculated curvature is included. (b) is the cross section when a 20 nm ripple function (period=4 mm) is also included. (c) is the cross section for a curvature, ripple and figure error corrected capillary. Models are for 1000 rays each.

we can determine that the maximum ripple amplitude for a radius of curvature $R = 68$ m and a spot size of about $5 \mu\text{m}$ is around 50 nm. There are clearly 5 rings in the far field of this capillary and so I modeled 5 ripples with 20 nm amplitude (slope error= $20 \mu\text{rad}$). The output for this model is available in Fig. 13(b). Notice that the widths of the ring in the far field do not change much but that the distribution of the rays changes significantly. The narrow part of the ring condenses into 2 intensity peaks, one wide and one narrow. When compared with the actual far field image of the capillary, this agrees quite well with what we see at the narrowest part of the ring. The wide part of the ring, surprisingly does not develop 5 intensity peaks as we expected from adding 5 ripples, rather we only see two peaks.

Finally, the figure error function was superposed on the capillary and the simulation was run with curvature, ripple and figure error (Fig. 13(c)). As compared with 13(b), the narrow part of the ring becomes even narrower and the intensity smears out such that we now see a more symmetric distribution. This distribution agrees very strongly with what we see in the far field image which essentially looks like one ring in the narrow region with a continuous distribution of intensity, however, the width of the ring is too narrow by a factor of 2. The wide part of the ring also changes significantly. The region becomes wider (although still differs from the expected width by 17%) and the five intensity peaks caused by the ripples are clearly visible. The differences between Figs. 13(b) and 13(c) suggest that certain amounts of curvature have the ability to reduce the visibility of ripples. This seems to be

due to the condensing of the ripple pattern – notice that the peaks in 13(b) are two bins wide while the peaks in 13(c) are only one bin wide. All five peaks in 13(c) are about the same intensity except for the peak furthest from the axis which appears to be somewhat brighter. It is difficult to tell from the far field image which peaks are brightest because of our limited resolution, however, it does appear that this seems to be one of the primary attributes of this model that differs significantly from our experimentally observed data⁷. Overall, the agreement between the model and the experimental data is very strong.

This model also proved to have strong agreement between the modeled focus and the experimentally observed focus. The focus of this capillary was estimated using a knife-edge scan to be $4.9 \times 5 \mu\text{m}$. The model yielded a minimum rms of $3.8 \mu\text{m}$ at 17mm. For a Gaussian distribution the rms is related to the full width half maximum (FWHM) by the relationship $\text{FWHM} \approx \text{RMS} * 1.36$ which would yield a FWHM spot size of about $5.2 \mu\text{m}$ which is in agreement with our measured value. Since the distribution at the focus of a curved capillary is not Gaussian, but skewed, this value must be adjusted somewhat.

6 Conclusions

My model indicates that an ideal capillary with a 1 mm source and a semi-major axis of about 17 m produces a spot size of $0.03\text{-}0.04 \mu\text{m}$. Any slope error significantly increases the spot size. As hypothesized, alternating bright and dark rings in the far field are due to periodic ripples on the inner surface of the capillary, and non-concentricity of innermost and outermost rings of the far field pattern are due to a banana-type curvature of the capillary itself. Increasing ripple amplitude or decreasing ripple wavelength, as well as decreasing the radius of curvature increases the rms spot size of the capillary. Adding a figure error correction to the capillary increases the spot size and shifts the focal spot further from the capillary tip.

Capillary G1_mr7f15_01 was successfully modeled to suitable accuracy using my simulation. As discussed in Section 5, it is difficult to determine which rings in our far field image are the brightest because we are limited by the spatial resolution of our x-ray screen and visible light viewing system. If we were capable of higher resolution imaging, the agreement between model output and the experimentally observed far field image could be better analyzed. Certainly the biggest disagreement between the model and the experimental data was that the widths of the ring in the model were quite a bit narrower than observed in experiment. It is possible this is because describing the curvature of the capillary by a single radius of curvature may not be sufficient.

The slight disagreement between the modeled widths of the far field rings and the observed widths of the far field. If figure error at the tip and curvature were dependent upon one another, it might explain why the more curved capillary G1_mr8f10_07 had a higher estimated figure error and yet still exhibited better performance. Certainly our current means of estimating figure error is not sufficient

⁷This result may in fact be an effect of the two-dimensional model. We are not sure how the distribution of intensity would change if the model were for three dimensions

since in the case of G1_mr7f15_01 it overestimated the figure error by a factor of 3 and in the case of G1_mr8f10_07 it overestimated the figure error by a factor of 4. For these two capillaries it was apparent that flattening the tip by more than .33% of its theoretical profile decreased the divergence of the capillary by an unreasonable amount.

Curvature appears to contribute most to increasing the beam size at the focus of the capillary. The spot size is related to curvature linearly by $\frac{1}{R}$ where R is the radius of curvature. Data shows that unless we are able to increase our radius of curvature to $R > 125$ m for low amplitude ripple (amplitude < 30 nm), we will not be able to achieve a spot size of $2.5 \mu\text{m}$ or less.

My research thus shows that there are two main areas on which we must focus. Firstly, we must work toward reducing the effects of capillary curvature as it seems to be the most limiting factor in achieving a $2 \mu\text{m}$ spot size. Secondly, further developing our understanding of figure error and its cause, as well as stabilizing the puller during scans in order to get more accurate readings is necessary to develop methods to reduce, or more ideally, eliminate figure errors in our capillaries.

7 Future Research

In terms of my simulation, my most immediate goal is to take this two-dimensional simulation with one-dimensional output and to extrapolate it to a three-dimensional simulation with two-dimensional output in order to model capillaries most realistically. This may be accomplished in MATLAB, but will most likely be done in BMAD upon the finalization of BMAD tools for reflecting off of arbitrary surfaces. I also plan on creating a GUI to be used on a web interface such that users can see how a capillary is expected to perform if it has some amount of a given defect parameter.

I would like to continue to attempt to model capillaries for which we have already collected data to determine the degree of agreement between the simulation's model and the experimentally observed data. I would like to model both good and bad capillaries, as I believe both would be illuminating to study. While good capillaries would help us to determine the degree of imperfections that can be sustained while still producing a good capillary, bad capillaries will help us to determine the nature of the imperfections themselves and the ways in which they affect capillary performance. I would additionally like to use my simulation in order to model capillaries with asymmetric figure errors on the top and bottom surfaces of the capillary.

We are continually attempting to improve our methods of metrology, and now it appears to be more important than ever that our measurements are as precise as possible and we are currently in the process of gathering information on our scanning instruments. A very natural next step would be to look at the drift data we have been collecting and see if any of the figure error curves I determined show up in these scans. In addition, it would be useful to attempt to measure the inner and outer diameters of the tip of a capillary in order to determine whether or not the fixed ratio is sufficiently preserved. There has also been talk of designing a capillary straightener in order to try to correct for the bending of capillaries.

8 Acknowledgements

Special thanks to Don Bilderback for advising my research and to Gavrielle Untracht for helping me learn MATLAB. Data used in this paper was collected at CHESS G1 hutch with help from Arthur Woll, Mark Pfeifer, Gavrielle Untracht and Tom Szebenyi. CHESS is supported by the National Science Foundation (NSF) and NIH-NIGMS via NSF grant DMR-0225180. Thanks also to the NSF for providing funding for my REU experience via grant PHY-0849885.

References

- [1] *Optics*, WWW Document, (<http://en.wikipedia.org/wiki/Optics>)
- [2] Sterling W. Cornaby, *The Handbook of X-Ray Single-Bounce Monocapillary Optics, Including Optical Design and Synchrotron Applications*. Cornell University, May 2008. WWW Document, (http://glasscalc.chess.cornell.edu/Cornaby_Capillary_Handbook_2008.pdf)
- [3] Gavrielle Untracht, *Experimentally Measuring Slope Errors of Capillary X-Ray Optics*. Cornell University, July 2010.

9 Appendix

A *capillary_bounce_05* Simulation User's Guide

The simulation `capillary_bounce_05` models a capillary in MATLAB defined by a set of parameters specified by the user. Many of these parameters can be copied straight from Rong Hwang's Capillary Profile Calculator. The user must also specify a set of anonymous functions that describe the shape of the capillary.

The body of the program operates on an overarching while-loop that is terminated when the user-specified number of rays have been launched and reflected from the capillary surface. The program shoots rays (defined by a linear function) with a random slope and y-intercept value in a specified range. The program selects the rays that intersect the capillary walls and reflects them by the law of reflection across the normal. It then stores arrays of values at the focus of the ellipse, as well as at specified locations in the far field, then plots the values as histograms.

The simulation has two primary uses: To produce output that can be compared with existing data in order to gather information about the inner surface of an already existing capillary, or to create a theoretical model of a capillary in order to formulate hypotheses about the performance of the capillary.

A.1 Adjustable Parameters and Modeling Your Capillary

The adjustable parameters available to the user are the following:

- `a`: The semi-major axis of the ellipse expressed in millimeters.
- `semi_minor_axis`: The semi-minor axis of the ellipse expressed in millimeters.
- `far_field_screen`: The distance from the tip of the capillary to the far field screen expressed in millimeters.
- `slit_size`: The size of your source expressed in millimeters.
- `energy`: The energy of the x-rays being focused expressed in keV.
- `capillary_length`: The length of the capillary expressed in millimeters.
- `focal_length`: The designed focal length of the capillary expressed in millimeters.
- `n`: The number of rays you want the simulation to use. This number determines when the while loop in the main method of the program will terminate. (Note: The use of more rays results in smoother and more accurate output. The simulation takes about 20 seconds per 100 rays.)
- `ripple_amp`: The amplitude of the inner surface ripple expressed in nanometers. If no ripple is desired set this constant to zero. Note: Ripples on upper and lower surfaces will always be in phase with each other.
- `ripple_number`: The number of ripples along the inside surface of the capillary.
- `ripple_phase`: The phase shift of the ripple expressed in radians.
- `curvature_switch`: Set to 1 if curvature is desired or 0 if no curvature is desired.
- `radius_of_curvature`: The radius of the circle that would be formed by extending the capillary expressed in meters.
- `Vo`, `Wo`, `Xo`, `Yo`, `Zo`: The coefficients of the quartic function $Vx^4 + Wx^3 + Xx^2 + Yx + Z$ which defines the figure error of the capillary. If a cubic function is preferred, set `Vo=0`. If no figure error is desired, all of these values should be set to zero.

A.2 Non-Adjustable Parameters

The non-adjustable-labeled parameters provided at the start of the script should not be modified. These values are a series of constants which are used frequently throughout the program. Non-adjustable parameters utilize the user's input from the "Adjustable Parameters" section and may simply change the units or alter the input such that it is in a more useful form.

A.3 Modifying Your Capillary

It is necessary that one specifies a set of anonymous functions that define the capillary and its defects – these functions are used as arguments to the “fminsearch” routine provided by MATLAB, which uses a numerical algorithm to find roots without having to take derivatives of the functions in question.

- `ellipse`: This function should not be altered as it specifies the fundamental shape of the capillary. The simulation is based on the geometry that one focus of the ellipse is at the origin of the coordinate system.
- `ripple`: This function is always sinusoidal and can be modified using the `ripple_amp`, `ripple_number` and `ripple_phase` constants in the “Adjustable Parameters” section. It specifies the periodic ripple that is a characteristic of the inner surface of imperfect capillaries.
- `curvature`: This function is a circular correction that describes how bent (like a banana) the capillary is. This function can be modified using the `radius_of_curvature` constant in the “Adjustable Parameters” section. The `radius_of_curvature` function should never be set to zero. If no curvature is desired, the curvature switch parameter `curvature_switch` must be set to zero⁸. If curvature *is* desired, the curvature switch should be set to 1.
- `figure_error`: This function is a quartic correction for the characteristic flattening of the tip of capillaries as a result of a systematic error of the puller. The coefficients for this function can be obtained using the supplementary script file `fig_err_analysis` (see section A.6) which reads in the data from the LabView capillary scans from a MATLAB text file and fits a cubic or quartic function to the difference between the theoretical and observed diameter profile.
- `noise`: This function can and should be modified in whatever way the user desires. This function can describe any other random noise that may either be expected or observed. When no additional noise is desired, enter the zero function. Suggestions for use: Gaussian curve, Fourier Decomposition.

The general form of an anonymous function is:

```
function_handle=@(arguments) (function).
```

As an example, the `ripple` function, which is a function of `x` and takes the arguments `A` (amplitude) and `ripple_k` (wave number) looks like

```
ripple=@(x,A,ripple_k) (A*sin(ripple_k*x)).
```

Thus when specifying a new anonymous function, all arguments must be included in the argument list in the right hand set of parenthesis, while the function itself must be specified in the left hand set of parenthesis. Be sure to define all new constants in the “Adjustable Parameters” list and to use the proper syntax when calling the noise function later in the program, that is, an anonymous function must always be called with all of its arguments, i.e. `noise(x, other arguments)`.

⁸This is because by setting the `radius_of_curvature` constant to zero you are actually telling the simulation that you want *infinite* curvature

A.4 Information Storage

There is a significant amount of storage already allotted in the program for arrays of values at various planes along the axis of the capillary. There is storage allotted for the plane of the focus of the capillary, and the far field, which is specified by the user. (Note: the far field should be greater than 700 mm to avoid redundancy). Additionally, there is storage allotted for 8 planes in the far field ranging from 50 mm from the ideal focus of the ellipse out to 700 mm from the ideal focus. Finally, there is storage for the pinhole scanning feature which scans the focus at 10 planes and calculates the rms value of the spot on each plane, then selects the plane with the smallest rms value as the focal plane of the capillary.

A.5 The Algorithm

The program begins by plotting the capillary determined by the user's input in a two-dimensional plane. The program also plots the ideal focus of the ellipse that defines the capillary, and the screen in the far field.

A while loop executes until a counter matches the input value n , the user's desired number of rays. While the counter is less than the input value n , the program launches a random ray defined by a linear function $y = mx + b$ where b is a parameter constrained by the size of the source and m is a parameter constrained by a reasonable range. The `fminsearch` MATLAB routine then executes until it locates the intersection, or root, of that ray with the capillary. The program selects and stores only the rays that actually intersect the capillary. All rays that either miss the capillary or go straight through the capillary are thrown out. When a root is found, the program then searches for the index of the root in the array of values that define the capillary surface. When the index is located, the x and y values at that index are stored as (x_2, y_2) and likewise the x and y values at the two adjacent indices are stored as (x_1, y_1) and (x_3, y_3) . The program then calculates the local slope and angle of incidence of the ray on the capillary at (x_2, y_2) . By a geometrical argument the ray is reflected off the capillary surface by the law of reflection which is accomplished by recalculating the new slope and y-intercept of the reflected ray. Finally, information about the y-displacement of rays is stored in cross-section arrays at various y displacements: the focus, the far field screen and at other desired cross sections along the axis of the capillary between the focus and beam stop. This information is then plotted in the form of histograms.

A.6 Using *fig_err_analysis*

The script file `fig_err_analysis` was developed to help determine figure error correction function coefficients to be used in `capillary_bounce_05`. To use `fig_err_analysis`, first import theoretical and observed data profiles for the capillary you wish to analyze into MATLAB as two separate text files. Be sure to delete all data that is not representative of the curve of the actual capillary (these files will contain data of the entire pull, but we are not interested in the whole pull). Specify the path

to each file in the program. Specify the capillary specs and the degree of polynomial you desire to fit – this will probably be a cubic function, then run the program⁹. Plot the function using an “ezplot” technique and make sure that the curve is reasonable. The output of the program is a vector of the coefficients of the polynomial correction function in decreasing numerical order (i.e. your correction function will be $Ax^3 + Bx^2 + Cx + D$). Note: it is likely you will need to adjust this function by a constant factor when you add it to the program.

A.7 Output and Data Analysis

A.7.1 Statistical Output

The `spot_size_rms` output value outputs the minimum rms value in microns of the focal spot, and is related to the FWHM value by the relationship $\text{FWHM} = \text{RMS} * 1.36$ for a Gaussian distribution. The FWHM value would be achieved by a pinhole scan of the focus¹⁰. The `expected_focal_length` is the value in millimeters of the distance of the capillary’s focus from the capillary’s tip.

A.7.2 Histograms

The simulation is capable of outputting three histogram plots which illustrate ray distributions in the far field at various cross sections, and a plot of 12 histograms that represent a scan across the focus of the capillary. These plots assist in visualization of the way the x-ray distribution changes at the focus and in the far field. They can also be compared to existing data and images in order to gain insight about the inner surface of the capillary. Any or all of these plots can be commented out without breaking the flow of the simulation.

A.7.3 Diagram

The simulation outputs a two-dimensional diagram of the capillary and the rays that were evaluated. This plot can be used to visualize the distribution of rays at and around the focus as well as the distributions of rays incident on the capillary.

B Source Code

```
1 close all;
2 clear;
3
4 hold on
```

⁹If you try to fit a cubic function and the resulting curve appears to be unreasonable, try a quartic function

¹⁰This value is adjusted such that it will output the correct rms value of the spot size even if the spot occurs off-axis.

```

5 axis([34990 35730 -3 3])
6
7 %Adjustable parameters
8 a=17515; %Enter desired semi-major axis (mm)
9 semi_minor_axis=1.1838896; %Enter desired semi-minor axis (mm)
10 far_field_screen=780; %Enter distance from capillary tip to screen (mm)
11 slit_size=1; %Enter size of slit (mm)
12 energy=10; %Enter energy of x-rays in keV
13 capillary_length=20; %Enter capillary length (mm)
14 focal_length=10; %Enter focal distance beyond capillary tip (mm)
15 n=300; %Enter desired number of light rays
16 ripple_amp=30; %Enter ripple amplitude in NANOMETERS
17 ripple_number=6; %Enter desired number of ripples along the inner surface of the capillary
18 ripple_phase=0; %Enter desired starting phase of ripple in radians
19 curvature_switch=1; %Enter 1 if you would like a curvature correction, or 0 if not
20 radius_of_curvature=60; %Enter desired radius of banana-type curvature (m)
21 %The following constants pertain to the figure error (cubic correction):
22 Vo=0;
23 Wo=0;
24 Xo=0;
25 Yo=0;
26 Zo=0;
27
28 %Non-adjustable parameters: DO NOT CHANGE!
29 critical_angle=.001*(32/energy); %critical angle in milliradians
30 e= sqrt(1-(semi_minor_axis/a)^2);
31 focus=2*a*e;
32 cap_base=focus-focal_length-capillary_length;
33 cap_tip=focus-focal_length;
34 bs=cap_tip+far_field_screen;
35 i=1;
36 index=0;
37 A=ripple_amp*10^-6;
38 ripple_k=2*pi*ripple_number/capillary_length;
39 R_banana=radius_of_curvature*10^3;
40 V=Vo*10^-3; %converts micron units in to millimeter units
41 W=Wo*10^-3;
42 X=Xo*10^-3;
43 Y=Yo*10^-3;
44 Z=Zo*10^-3;
45
46 %%%Define the functions that describe the capillary%%
47 ellipse=@(x,a,e)(sqrt((1-e^2)*(a^2-(x-a*e).^2))); %Do not change this one

```



```

48 ripple=@(x,A,ripple_k,ripple_phase)(A*sin(ripple_k*x+ripple_phase)); ...
49     %Periodic correction
50 curvature=@(x,R_banana,cap_base)(curvature_switch*...
51     (-R_banana+sqrt(R_banana^2-(x-cap_base).^2)); %Circular correction
52 figure_error=@(x)(V*(x-cap_base).^4+W*(x-cap_base).^3...
53     +X*(x-cap_base).^2+Y*(x-cap_base)+Z); %Cubic/Quartic correction given...
54                                     %by output of 'fig-err-analysis'
55 noise=@(x)(0); %arbitrary correction
56
57 %Storage for far field and focus cross sections
58 far_field_position=zeros(1,n);
59
60 %storage for FWHM pinhole scans
61 plane=focus-3:1:focus+8;
62 focal_scan=zeros(12,n);
63 focus_rms=zeros(1,12);
64 CoM_spot=zeros(1,12);
65
66 %Storage for additional cross sections
67 farfield500=zeros(1,n);
68 farfield600=zeros(1,n);
69 farfield700=zeros(1,n);
70
71 nearfield50=zeros(1,n);
72 nearfield100=zeros(1,n);
73 nearfield200=zeros(1,n);
74 nearfield300=zeros(1,n);
75 nearfield400=zeros(1,n);
76
77 %%%%%%%%%%%%%%%%%%%%%%%%%%%%%%%%%%%%%%%%%%%%%%%%%%%%%%%%%%%%%%%%%%%%%%%%%
78 %program begins here
79 %%%%%%%%%%%%%%%%%%%%%%%%%%%%%%%%%%%%%%%%%%%%%%%%%%%%%%%%%%%%%%%%%%%%%%%%%
80
81 %%%create environment%%%%%%%%%%
82 %draws the capillary
83 x=linspace(cap_base,cap_tip,100);
84 y_pos=sqrt((1-e^2)*(a^2-(x-a*e).^2))+ripple(x,A,ripple_k,ripple_phase)...
85     +curvature(x,R_banana,cap_base)+figure_error(x)+noise(x);
86 y_neg=-sqrt((1-e^2)*(a^2-(x-a*e).^2))+ripple(x,A,ripple_k,ripple_phase)...
87     +curvature(x,R_banana,cap_base)-figure_error(x)+noise(x);
88
89 xx_capillary=cap_base:.001:cap_tip;
90 yy_capillary_pos=spline(x,y_pos,xx_capillary);

```

```

91 yy_capillary_neg=spline(x,y_neg,xx_capillary);
92
93 plot(xx_capillary, yy_capillary_pos,xx_capillary,yy_capillary_neg)
94 plot(focus,0,'b+') %the focus of the ellipse
95
96 %draws the beamstop
97 x=bs*ones(100,1)+.01;
98 y=linspace(-5,5,100);
99 plot(x,y, 'g-')
100
101 %%%%%%%%%%%%%%%%%%%%%%%%%%%%%%%%%%%%%%%%%%%%%%%%%%%%%%%%%%%%%%%%%%%%%%%%%
102 while i<=n;
103     %generate a random ray
104     m=.000005*(2*rand(1)-1);
105     b=.5*slit_size*(2*rand(1)-1);
106
107 %set options for fminsearch
108 options=optimset('Display','off','MaxIter',100000,'TolFun',.00000001,...
109     'TolX',.0000001);
110
111     if m>0
112         func=@(x) (abs(-(m*x+b))+ellipse(x,a,e)+ripple(x,A,ripple_k,ripple_phase)...
113             +curvature(x,R_banana,cap_base)+figure_error(x)+noise(x));
114     elseif m<0
115         func=@(x) (abs(-(m*x+b))-ellipse(x,a,e)+ripple(x,A,ripple_k,ripple_phase)...
116             +curvature(x,R_banana,cap_base)-figure_error(x)+noise(x));
117     elseif m==0
118         if b>0
119             func=@(x) (abs(-(m*x+b))+ellipse(x,a,e)+ripple(x,A,ripple_k,ripple_phase)...
120                 +curvature(x,R_banana,cap_base)+figure_error(x)+noise(x));
121         else
122             func=@(x) (abs(-(m*x+b))-ellipse(x,a,e)+ripple(x,A,ripple_k,ripple_phase)...
123                 +curvature(x,R_banana,cap_base)-figure_error(x)+noise(x));
124         end
125     end
126     %find the intersection of the ray and capillary
127     root=fminsearch(func,cap_tip-.5*capillary_length,options);
128     function_value=m*root+b;
129
130     if root<cap_tip-.001 && root>cap_base+.001
131         %if the root is within the bounds of the capillary...
132
133     %search the ellipse for the INDEX of intersection

```

```

134 [rows, columns] = size(xx_capillary);
135 for k=2:columns
136     if xx_capillary(k-1)<root && xx_capillary(k)>root;
137         %if the value of the index==root
138         index=k; % store the index
139     end
140 end
141 if index==0; %if an index is not stored, throw out this ray
142     i=i-1;
143 else
144     x1=xx_capillary(index-1);
145     x2=xx_capillary(index);
146     x3=xx_capillary(index+1);
147
148     %if the function value is positive it intersects the positive half of
149     % the capillary
150     if function_value>0
151         y1=yy_capillary_pos(index-1);
152         y2=yy_capillary_pos(index);
153         y3=yy_capillary_pos(index+1);
154
155     %if the function value is negative it intersects the bottom half of
156     %the capillary
157     else
158         y1=yy_capillary_neg(index-1);
159         y2=yy_capillary_neg(index);
160         y3=yy_capillary_neg(index+1);
161     end
162
163     %find the angle of incidence by calculating the local slope at
164     % (x2,y2)
165     [theta_incident, alpha, phi]=find_angle_of_incidence(x1,y1,x2,y2,x3,y3,m);
166
167     if abs(theta_incident)<critical_angle %may be unnecessary
168
169         %plot the ray
170         ray_x=linspace(0,root,100);
171         ray_y=m*ray_x+b;
172         plot(ray_x,ray_y,'r')
173
174         %reflect the ray by the law of reflection
175         [reflected_x, reflected_y, reflected_ray_slope,...
176         reflected_ray_intercept] = reflect_ray_02(theta_incident,...

```

```

177     alpha, root, function_value, bs);
178     plot(reflected_x, reflected_y, 'r')
179
180     %obtain the y value of the reflected ray at the beamstop
181     far_field_position(i)=reflected_y(100);
182
183     %obtain y values at focal scans
184     for r=1:12
185         focal_scan(r,i)=reflected_ray_slope*plane(r)+reflected_ray_intercept;
186     end
187
188     %obtain y values at additional cross sections
189     nearfield50(i)=reflected_ray_slope*(focus+50)+reflected_ray_intercept;
190     nearfield100(i)=reflected_ray_slope*(focus+100)+reflected_ray_intercept;
191     nearfield200(i)=reflected_ray_slope*(focus+200)+reflected_ray_intercept;
192     nearfield300(i)=reflected_ray_slope*(focus+300)+reflected_ray_intercept;
193     nearfield400(i)=reflected_ray_slope*(focus+400)+reflected_ray_intercept;
194     farfield500(i)=reflected_ray_slope*(focus+500)+reflected_ray_intercept;
195     farfield600(i)=reflected_ray_slope*(focus+600)+reflected_ray_intercept;
196     farfield700(i)=reflected_ray_slope*(focus+700)+reflected_ray_intercept;
197
198     else
199         i=i-1;
200     %catches the rays that have incident angles greater than the critical angle
201     end
202 end
203
204 else %this code catches the rays that hit the ellipse at an x value
205     %greater than the x value of the focal point and throws them out
206     i=i-1;
207 end
208
209 i=i+1; %increment the while loop
210 end
211
212 %store positive and negative values in the far field
213 q=find(far_field_position>0);
214 r=find(far_field_position<0);
215
216 far_field_pos=far_field_position(q);
217 far_field_neg=far_field_position(r);
218
219 %store positive and negative values of additional far field cross sections

```

```

220 q500=find(farfield500>0);
221 r500=find(farfield500<0);
222 ff500_pos=farfield500(q500);
223 ff500_neg=farfield500(r500);
224
225 q600=find(farfield600>0);
226 r600=find(farfield600<0);
227 ff600_pos=farfield600(q600);
228 ff600_neg=farfield600(r600);
229
230 q700=find(farfield700>0);
231 r700=find(farfield700<0);
232 ff700_pos=farfield700(q700);
233 ff700_neg=farfield700(r700);
234
235 q50=find(nearfield50>0);
236 r50=find(nearfield50<0);
237 nf50_pos=nearfield50(q50);
238 nf50_neg=nearfield50(r50);
239
240 q100=find(nearfield100>0);
241 r100=find(nearfield100<0);
242 nf100_pos=nearfield100(q100);
243 nf100_neg=nearfield100(r100);
244
245 q200=find(nearfield100>0);
246 r200=find(nearfield100<0);
247 nf200_pos=nearfield100(q100);
248 nf200_neg=nearfield100(r100);
249
250 q300=find(nearfield100>0);
251 r300=find(nearfield100<0);
252 nf300_pos=nearfield100(q100);
253 nf300_neg=nearfield100(r100);
254
255 q400=find(nearfield100>0);
256 r400=find(nearfield100<0);
257 nf400_pos=nearfield100(q100);
258 nf400_neg=nearfield100(r100);
259
260 %simulates a pinhole scan and calculates rms of the focus as well as
261 %the focal length
262 figure

```

```

263 for k=1:12
264     CoM_spot(k)=sum(focal_scan(k,1:n)/n);
265     focus_rms(k)=10^3*sqrt(sum((focal_scan(k,1:n)-CoM_spot(k)).^2)/n);
266     subplot(3,4,k)
267     hist(focal_scan(k,1:n),30)
268     h(k)=findobj(gca,'Type','patch');
269     set(h(k),'Facecolor','r','EdgeColor','w')
270
271 end
272 spot_size_rms=min(focus_rms)
273 ind=find(focus_rms==spot_size_rms);
274 expected_focal_length=plane(ind)-cap_tip
275 position_at_focus=focal_scan(ind,1:n);
276
277 %plot for focus and far field cross sections
278 figure
279     hold on
280     subplot(3,1,1)
281     hist(position_at_focus,30)
282     h=findobj(gca,'Type','patch');
283     set(h,'FaceColor','r','EdgeColor','w')
284     title('Distribution of Rays at Focus of Capillary')
285
286     subplot(3,1,2)
287     hist(far_field_pos,30)
288     h=findobj(gca,'Type','patch');
289     set(h,'FaceColor','r','EdgeColor','w')
290     title('Distribution on Far Field screen (+)')
291
292     subplot(3,1,3)
293     hist(far_field_neg,30)
294     h=findobj(gca,'Type','patch');
295     set(h,'FaceColor','r','EdgeColor','w')
296     title('Distribution on Far Field Screen(-)')
297
298
299 %near field plots
300 figure
301     hold on
302     subplot(2,4,1)
303     hist(nf50_pos,30)
304     h=findobj(gca,'Type','patch');
305     set(h,'FaceColor','r','EdgeColor','w')

```

```

306 title('Distribution in Near Field (50mm, +)')
307
308 subplot(2,4,2)
309 hist(nf100_pos,30)
310 h=findobj(gca,'Type','patch');
311 set(h,'FaceColor','r','EdgeColor','w')
312 title('Distribution in Near Field (100mm, +)')
313
314 subplot(2,4,3)
315 hist(nf200_pos,30)
316 h=findobj(gca,'Type','patch');
317 set(h,'FaceColor','r','EdgeColor','w')
318 title('Distribution in Near Field (200mm, +)')
319
320 subplot(2,4,4)
321 hist(nf300_pos,30)
322 h=findobj(gca,'Type','patch');
323 set(h,'FaceColor','r','EdgeColor','w')
324 title('Distribution in Near Field (300mm, +)')
325
326 subplot(2,4,5)
327 hist(nf50_neg,30)
328 h=findobj(gca,'Type','patch');
329 set(h,'FaceColor','r','EdgeColor','w')
330 title('Distribution in Near Field (50mm, -)')
331
332 subplot(2,4,6)
333 hist(nf100_neg,30)
334 h=findobj(gca,'Type','patch');
335 set(h,'FaceColor','r','EdgeColor','w')
336 title('Distribution in Near Field (100mm, -)')
337
338 subplot(2,4,7)
339 hist(nf200_neg,30)
340 h=findobj(gca,'Type','patch');
341 set(h,'FaceColor','r','EdgeColor','w')
342 title('Distribution in Near Field (200mm, -)')
343
344 subplot(2,4,8)
345 hist(nf300_neg,30)
346 h=findobj(gca,'Type','patch');
347 set(h,'FaceColor','r','EdgeColor','w')
348 title('Distribution in Near Field (300mm, -)')

```

```

349
350 %midfield plots
351 figure
352 hold on
353     subplot(2,4,1)
354     hist(nf400_pos,30)
355     h=findobj(gca,'Type','patch');
356     set(h,'FaceColor','r','EdgeColor','w')
357     title('Distribution in Near Field (400mm, +)')
358
359     subplot(2,4,2)
360     hist(ff500_pos,30)
361     h=findobj(gca,'Type','patch');
362     set(h,'FaceColor','r','EdgeColor','w')
363     title('Distribution in Far Field (500mm, +)')
364
365     subplot(2,4,3)
366     hist(ff600_pos,30)
367     h=findobj(gca,'Type','patch');
368     set(h,'FaceColor','r','EdgeColor','w')
369     title('Distribution in Far Field (600mm,+)')
370
371     subplot(2,4,4)
372     hist(ff700_pos,30)
373     h=findobj(gca,'Type','patch');
374     set(h,'FaceColor','r','EdgeColor','w')
375     title('Distribution in Far Field (700mm,+)')
376
377     subplot(2,4,5)
378     hist(nf400_neg,30)
379     h=findobj(gca,'Type','patch');
380     set(h,'FaceColor','r','EdgeColor','w')
381     title('Distribution in Near Field (400mm, -)')
382
383     subplot(2,4,6)
384     hist(ff500_neg,30)
385     h=findobj(gca,'Type','patch');
386     set(h,'FaceColor','r','EdgeColor','w')
387     title('Distribution in Far Field (500mm,-)')
388
389     subplot(2,4,7)
390     hist(ff600_neg,30)
391     h=findobj(gca,'Type','patch');

```



```

392     set(h, 'FaceColor', 'r', 'EdgeColor', 'w')
393     title('Distribution in Far Field (600mm,-)')
394
395     subplot(2,4,8)
396     hist(ff700_neg,30)
397     h=findobj(gca, 'Type', 'patch');
398     set(h, 'FaceColor', 'r', 'EdgeColor', 'w')
399     title('Distribution in Far Field (700mm,-)')

```

```

1  function [angle_of_incidence,alpha,phi ] = ...
2      find_angle_of_incidence(x1,y1,x2,y2,x3,y3,slope_ray_in )
3  %This function calculates the angle of incidence of the ray on the capillary based on the l
4
5  %find the slope between points:
6  m12=(y2-y1)/(x2-x1);
7  m23=(y3-y2)/(x3-x2);
8
9  slope_x2y2=.5*(m12+m23);
10
11 alpha=atan(slope_ray_in);
12 phi=-atan(slope_x2y2);
13
14 angle_of_incidence=phi+alpha;
15
16 end

```

```

1  function [ray_out_x, ray_out_y,m_reflected_ray, b_reflected_ray ] =...
2      reflect_ray_02(angle_of_incidence,alpha,root,y_at_root,beamstop_location)
3
4  %This function reflects the incident ray by the law of reflection
5
6  xi=2*angle_of_incidence-alpha;
7
8  m_reflected_ray=-tan(xi);
9  b_reflected_ray=y_at_root-m_reflected_ray*root;
10
11 ray_out_x=linspace(root,beamstop_location,100);
12 ray_out_y=m_reflected_ray*ray_out_x+b_reflected_ray;
13
14 %plot(ray_out_x, ray_out_y, 'r')
15

```

16 **end**

```
1  %%This code calculates the cubic correction necessary to account for
2  %%capillary figure error at the tip. Delete all values from data file
3  %%that do not directly correspond to the capillary profile
4
5  clear;
6  close all;
7
8  [text_file, tpath]=uigetfile('*.txt');
9  Sp1=regexp(text_file, '_');
10 Sp2=regexp(text_file, '\. ');
11 capillary_name=text_file(1:Sp2-1);
12
13 %Enter pathway to observed data
14 observed_values= %ENTER PATH
15
16 A=load(observed_values);
17
18 %Enter pathway to theoretical data
19 theoretical_values=%ENTER PATH
20 B=load(theoretical_values);
21
22 z_obs=A(:,1)-30;
23 z_theo=B(:,1)-30;
24
25 diam_obs=A(:,2);
26 diam_theo=B(:,2);
27
28 radius_obs=diam_obs./2;
29 radius_theo=diam_theo./2;
30
31 %fits a cubic function to the data
32 poly_obs=polyfit(z_obs, radius_obs, 3);
33 poly_theo=polyfit(z_theo, radius_theo, 3);
34
35 %stores the cubic function in arrays
36 xi_obs=linspace(0, 20, 202);
37 yi_obs=polyval(poly_obs, z_obs);
38
39 xi_theo=linspace(0, 20, 2001);
40 yi_theo=polyval(poly_theo, z_theo);
```

41

42 *%calculates the necessary data correction and outputs it*

43 `fig_err_correction=poly_obs-poly_theo`